Nonlinear Processes in Geophysics (2000) 7: 173–177

Nonlinear Processes in Geophysics

On a nonlinear state of the electromagnetic ion/ion cyclotron instability

M. Cremer[1] and M. Scholer[1,2]

[1]Max-Planck-Institut für Extraterrestrische Physik, 85740 Garching, Germany
[2]STEL, Nagoya University, Toyokawa 442, Japan

Received: 22 November 1999 – Revised: 22 March 2000 – Accepted: 7 April 2000

Abstract. We have investigated the nonlinear properties of the electromagnetic ion/ion cyclotron instability (EMIIC) by means of hybrid simulations (macroparticle ions, massless electron fluid). The instability is driven by the relative (super-Alfvénic) streaming of two field-aligned ion beams in a low beta plasma (ion thermal pressure to magnetic field pressure) and may be of importance in the plasma sheet boundary layer. As shown in previously reported simulations the waves propagate obliquely to the magnetic field and heat the ions in the perpendicular direction as the relative beam velocity decreases. By running the simulation to large times it can be shown that the large temperature anisotropy leads to the ion cyclotron instability (IC) with parallel propagating Alfvén ion cyclotron waves. This is confirmed by numerically solving the electromagnetic dispersion relation. An application of this property to the plasma sheet boundary layer is discussed.

1 Introduction

Relative streaming of ions has been observed to occur in the plasmasheet boundary layer (DeCoster and Frank, 1979; Elphic and Gary, 1990), and it is expected that this source of free energy gives rise to plasma instabilities and to associated waves. Gary and Winske (1990) have investigated the ion cyclotron anisotropy instability driven by a temperature anisotropy of the individual ion components, and the proton/proton nonresonant instability driven by the free energy in the relative streaming between the two ion components. They have used both linear theory and one-dimensional computer simulations to study instability growth and saturation and concluded that both instabilities yield only weak proton scattering. Since they were interested in identifying the mode that converts the counterstreaming ions into a single, isotropic velocity shell distribution they excluded these instabilities as a possible cause. A somewhat different instability has been proposed by Winske and Omidi (1990; 1992) in connection with dissipation at slow shocks in the magnetotail and ion heating in the plasmasheet boundary layer. This so-called electromagnetic ion/ion cyclotron instability (EMIIC) is also driven by the relative streaming of two field-aligned ion beams. The instability has its origin in the ion beam driven electrostatic instability (Weibel, 1970; Miura et al., 1983); however, in a finite beta plasma the instability is electromagnetic and has rather different properties. The mode extends from the ion cyclotron branch at frequencies below the ion gyrofrequency to the shear Alfvén branch above the ion cyclotron frequency, and maximum growth is at oblique angles. At almost perpendicular propagation the mode retains its ion cyclotron like character, but for a large range of oblique angles the mode is Alfvén like. The waves are linearly polarized and have a large electrostatic component.

Winske and Omidi (1992) have carried out a large number of hybrid simulations and have studied the linear and nonlinear properties. Most of these simulations were done in one dimension. At the end of the simulations they obtained an asymptotic state which was marginally stable. In addition they presented some two-dimensional simulations and have concluded that also in two dimensions the simulations result in a final state, which is quasi-linearly stable.

Recently Daughton et al. (1999) performed two-dimensional hybrid simulations of the EMIIC instability for several sets of parameters to find scaling relations for the individual component anisotropies. These relations show an increase of the upper bound on the relative anisotropies with decreasing core-β. For the range of β-values examined in their simulations these maximum relative anisotropies stay below the anisotropy threshold for excitation of the IC instability. It was suggested by Daughton et al. (1999) that the anisotropy due to perpendicular heating by the EMIIC instability might eventually exceed the IC-threshold for smaller values of β than examined.

In the present report we want to take up the problem of the nonlinear evolution of the electromagnetic ion/ion cyclotron instability. We present a two-dimensional hybrid simulation

Correspondence to: M. Scholer

and we will show that for the parameters investigated here the EMIIC instability does not saturate at oblique angles, but instead the final quasi-steady wave spectrum is dominated by parallel propagating waves. We will argue that perpendicular heating due to the EMIIC instability in the plasmasheet boundary layer will lead to parallel propagating Alfvén ion cyclotron waves.

2 Simulation model and results

The simulations are done with a two-dimensional hybrid code with macroparticle ions and an inertialess electron fluid. Details of the code can be found in the paper by Matthews (1994). The electron fluid is assumed to have a finite, but isotropic pressure, which follows an isothermal law. All variables are functions of time t and two variables x and z. The time is expressed in units of the inverse of the ion gyrofrequency $\Omega_{gi} = eB_o/m$, where e is the magnitude of the electron charge, m the ion mass, and B_o the constant magnetic field (in the x direction). Distances are expressed in units of the ion inertial length $\lambda_o = c/\omega_{pi}$ (c is speed of light, ω_{pi} is ion plasma based on the total ion density). The unit velocity is then the Alfvén velocity v_A, the number density is normalized to the total density n_o. Two ion beams are assumed to move parallel to the magnetic field in opposite directions. The simulations are done in a frame where the ion current is zero, i.e., in the rest frame of the electrons. Periodic boundary conditions are imposed in both the x and z direction. The system size is $0 \le L_x \le 64\lambda_o$, $0 \le L_x \le 64\lambda_o$ with a grid size of $\Delta x = \Delta z = 0.32\lambda_o$. The number of particles is 64 per cell. For comparison, Winske and Omidi (1992) used for their largest simulation a system size of $48\lambda_o \times 48\lambda_o$. In the first run we assume that both beams have the same density $n_j = 0.5n_o$ and that they move in the electron rest frame with a speed of v_A in opposite directions parallel to the magnetic field. The index $j = 1, 2$ distinguishes between the two ion components. The beams are initially isotropic Maxwellians with a plasma beta of $\beta_j = 0.07$ (ion thermal to magnetic field pressure: $\beta_j = 2\mu_o n_o k T_{\|\,j}/B^2$). In a second run we consider the case of a core distribution and a low density beam.

The assumption of equal beam densities in the first run seems to make application to the plasmasheet boundary layer somewhat questionable. However in simulations of the Riemann problem of the collapse of a current sheet with a superposed normal magnetic field component large densities of backstreaming ions in the boundary layer have indeed been found. Two-dimensional simulations of this Riemann problem have recently been reported by Cremer and Scholer (1999). Here we want first to present results of such a Riemann problem, where a 1-D (Harris-type) current sheet with a superposed normal field of $B_z = -0.15B_o$ of the outside magnetic field has been allowed to collapse. The ion beta outside the initial current sheet was assumed to be $\beta_i = 0.02$.

Figure 1 shows in the upper panel a spatial profile perpendicular to the current sheet of the bulk velocity of the backstreaming ions. The lower panel shows a profile of the density of the backstreaming ions, where the density is normalized to the local electron density. The parameters are only shown for $z > 20\lambda_o$ (the initial current sheet is symmetric to $z = 0$), since separation between backstreaming ions and heated lobe ions becomes impossible for distances smaller than $20\lambda_o$. It can be seen that the backstreaming ions have a density of up to 60% of the total density and that they are streaming with about twice the local Alfvén speed parallel to the magnetic field.

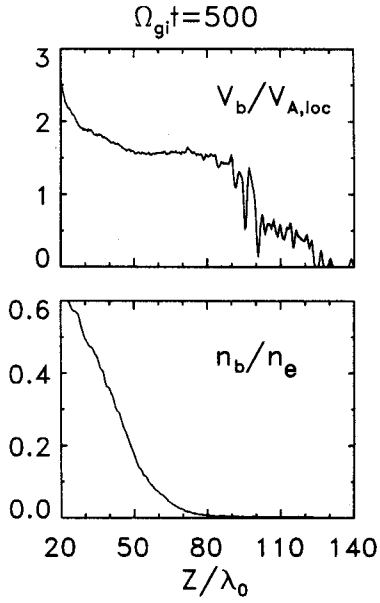

Fig. 1. Results from the simulation of the Riemann problem of the collapse of a current sheet: spatial profiles in the direction perpendicular to the current sheet of (upper panel) beam velocity v_b relative to local Alfvén speed $v_{A,loc}$ and (lower panel) of beam density n_b relative to total density n_e at timestep $t\Omega_{gi} = 500$.

Figure 2 shows the result of the EMIIC simulation for the equal density case (first run). Shown is the temporal development of the following parameters: (upper left panel) perpendicular (solid line) and parallel (dashed line) temperature of one beam, (lower left panel) bulk speed parallel to the average magnetic field, (upper right panel) energy density in the three magnetic field components B_y (solid line), B_z (dashed-dotted line), and B_x (dashed line), (lower right panel) energy density in two electric field components. Note that we have run the simulation up to $t\Omega_{gi} = 400$, i.e., twice as long as Winske and Omidi (1992). The initial development is rather similar to that obtained by Winske and Omidi in their larger 2-D run. δB_y^2 rises exponentially in the linear phase (up to $t\Omega_{gi} \sim 50$) to a maximum. Most of the wave energy density is in B_y and the waves are linearly polarized. The beams are exponentially slowed down. Following the linear stage the magnetic energy density decreases while the electric energy density continuously increases up to $t\Omega_{gi} \sim 150$. Up to this time the perpendicular temperature rapidly increases; after $t\Omega_{gi} \sim 200$ the temperature anisotropy is about constant, while the beams are slowed down further.

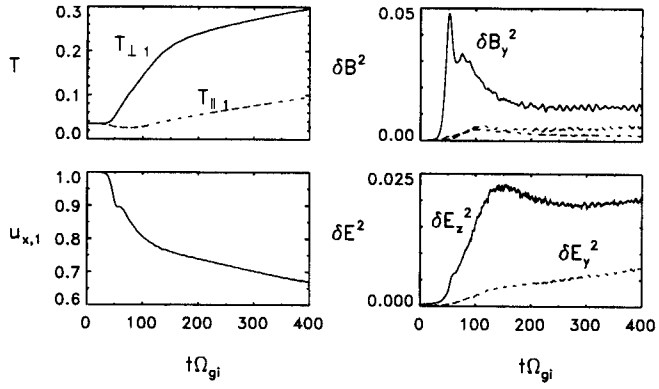

Fig. 2. Time histories of (upper left panel) $T_{\perp 1}$ solid line and $T_{||1}$ (dashed line), (upper right panel) δB_y^2 (solid line), δB_z^2 (dashed line), and δB_x^2 (dashed-dotted line), (lower left panel) bulk speed of beam 1, and (lower right panel) δE_z^2 and δE_y^2.

Figure 3 shows details of the wave structure during various phases of the instability. Shown are two-dimensional plots $(k_z - k_x)$ of the Fourier mode spectral density of one magnetic field component, δB_y. At the end of the linear phase and during the nonlinear phase the modes are concentrated at oblique angles θ_{kB} relative to the magnetic field. In the linear phase θ_{kB} is close to 70° as predicted by linear theory. After $t\Omega_{gi} \sim 200$ the modes are more and more concentrated at parallel propagation and move to slightly larger wavelenghts. Winske and Omidi (1992) did not follow their run into this regime. We will argue in the following that the EMIIC instability does not reach an asymptotic state as far as saturation at oblique angles is concerned, but that the final phase is dominated by the ion cyclotron instability. This instability is driven unstable by a $T_\perp > T_{||}$ anisotropy. Although at $t\Omega_{gi} \sim 200$ $T_\perp/T_{||}$ of the whole distribution is smaller than one, the instability can be driven by the temperature ansotropy of the individual components (e.g., Gary and Winske, 1990).

To this end we show in Figure 4 (left) the result of a two-dimensional Fourier transformation of the power in B_y for parallel propagating waves $\theta_{kB} = 0$ in the $\omega - k_x$ plane. The time interval for this study is $200 \leq \Omega_{gi}t \leq 400$. Also shown are the real frequency (solid line) and the growth rate (dashed line) as obtained by numerically solving the electromagnetic linear dispersion equation for a plasma consisting of of two beams with a temperature anisotropy approximated by bi-Maxwellian distributions. The temperature anisotropy is assumed to be $T_\perp/T_{||} = 5$ and the relative velocity of the two beams is assumed to be $1.5v_A$, as obtained at $t\Omega_{gi} \sim 200$ from the EMIIC simulation. Furthermore, in linear theory we have assumed that $\Omega_{gi}/\omega_{pi} = 10^{-4}$. There is in addition a branch with negative phase velocity not shown here. Linear theory predicts instability with k of maximum growth at $k_{max}\lambda_o = 0.8$. This is higher than the value obtained in the simulation. However, the parallel temperature continuously increases during the run so that the position of maximum growth moves to smaller k values, while changes in the dispersion relation $\omega(k_x)$ are relativley minor. The right-

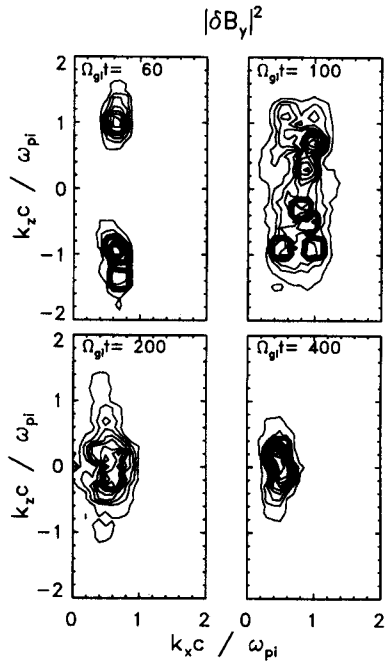

Fig. 3. Results of two-dimensional Fourier transformation of B_y at four different times.

hand part of Fig. 4 shows a hodogram of the magnetic field in the $B_y - B_z$ plane at one position in space during the time period $363 < \Omega_{gi}t < 385$. Since the average magnetic field points in the positive x direction the polarization is left handed.

We now present results from the second run for the case of a relatively low beam density of 25% of the total density. All other parameters are identical to those used in the first simulation.

Figure 5 shows the spatial evolution of various parameters; the index 1 stands for the beam component and the index 2 for the core component. The double peak structure of δB_y^2 has been interpreted by Winske and Omidi (1992) in terms of trapping of the beam particles. The maximum magnetic field energy density is by about a factor two lower compared to the case with beams of equal density. The maximum temperature anisotropy of ~ 6 of the beam is reached at $\Omega_{gi}t = 150$; sub-

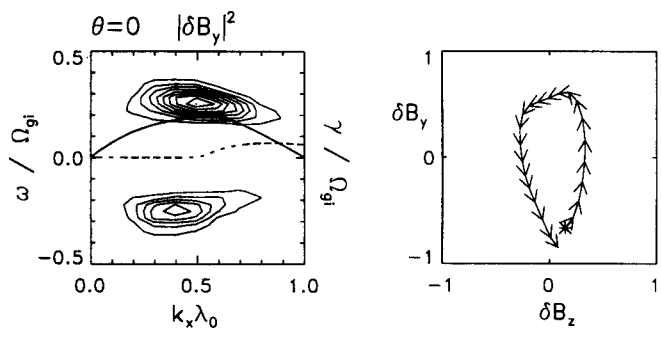

Fig. 4. (Left) wave spectrum for parallel propagating waves during $\Omega_{gi}t = 200$ and $\Omega_{gi}t = 400$; (Right) polarization of a wave train.

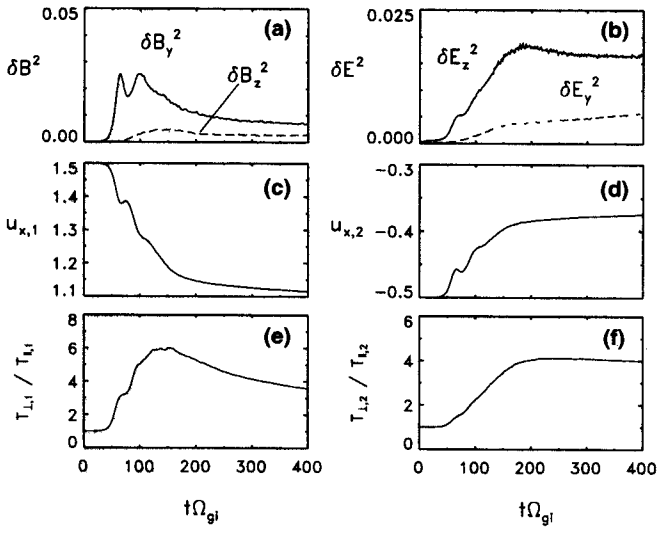

Fig. 5. Time histories of (upper left panel) δB_y^2 (solid line), δB_z^2 (dashed line), and δB_x^2 (dashed-dotted line), (upper right panel) δE_z^2 and δE_y^2, (middle panels) beam (index 1) and core (index 2) velocities, (lower left panels) beam and core temperature anisotropies.

sequently, the temperature anisotropy decreases. The core distribution reaches a lower anisotropy of ~ 4 and the value stays constant. The ion cyclotron instability due to the beam anisotropy alone has a considerably larger growth rate than instability due to the core anisotropy. It is thus expected that only the beam ions are resonant with the AIC waves and the anisotropy of the beam will decrease.

Figure 6 shows two-dimensional plots ($k_z - k_x$) of the Fourier mode spectral density of δB_y for the lower beam density case. As expected from linear theory the propagation of the EMIIC waves is more oblique and the wavelenghth is slighly smaller. After $\Omega_{gi}t \sim 150$, i.e., when the maximum growth rate for the ion cyclotron instability is reached, the wave vectors are predominatly in the direction parallel to the magnetic field.

3 Summary

By running the 2-D simulation of the EMIIC instability twice as long as has been done previously we have shown that this instability does not necessarily ever reach an asymptotic state as far as saturation at oblique angles is concerned. Energy from the relative velocity of the beams is transferred into perpendicular temperature of the individual beams. This allows for destabilization of the ion cyclotron temperature anisotropy instability at least for the parameters chosen in the present study. Indeed, the final state is characterized by parallel propagating Alfvén ion cyclotron waves. We thus have demonstrated explicitely that transition from the EMIIC instability to the IC instability takes place for the case of an initially small enough component-β, as was suggested by Daughton et al. (1999). As to the observed distribution functions in the plasma sheet boundary layer, Gary and Winske (1990) have concluded from 1-D simulations that they cannot be produced by the ion cyclotron instability, since pitch angle scattering by this instability is too weak. When applied to the plasma sheet boundary layer the results of the present $2D$-simulations point towards the fact that the simultaneous observations of low frequency waves and distribution functions need not necessarily imply a direct correlation between these two features. In fact, the form of the distribution function at the end of the simulation is a combined effect of both, the EMIIC instability and the IC instability, while the wave spectrum solely manifests parallel propagating ion cyclotron waves. But undoubtedly, aside from the changes due to the latter waves, the EMIIC instablity is responsible for a great deal of change of the distribution function. This must be kept in mind when connecting simultaneous observations of the particle distribution function and low-frequency waves.

It might be suggested from the results of our simulations, that the plasma sheet boundary layer will be dominated by parallel propagating ion cyclotron waves. Several caveats

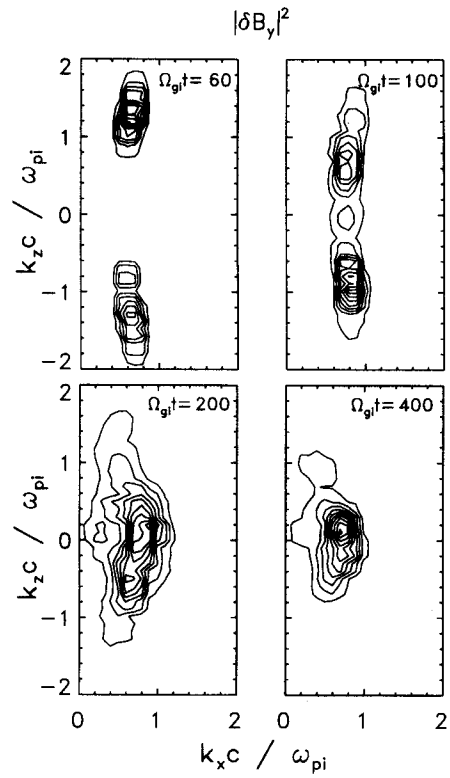

Fig. 6. Results of two-dimensional Fourier transformation of B_y at four different times (low beam density case).

are in place, however, when applying this to the plasma sheet boundary layer. The present investigation is not fully appropriate for addressing the plasma sheet boundary layer properly since one important property is missing: a continuous injection of backstreaming ions which corresponds to a driving of the EMIIC instability, whereas the present simulations represent an initial value problem. It is known that the question, which waves are dominant, is intimately linked to the details of the injection source. As a first step, though, towards more sophisticated models of the plasma sheet bound-

ary layer, the intention of this study was to isolate wave growth and evolution from directly driven effects which can obscure concurrent processes.

Nevertheless, we argue in favour of the dominace of parallel propagating ion cyclotron waves in the plasma sheet boundary layer. This view is supported by Fig. 7 in Daughton et al. (1999) and by the following reasoning. Once the threshold for the IC instability is exceeded due to perpendicular heating by the EMIIC instability, parallel propagating ion cyclotron waves will be excited. Pitch angle scattering by these waves leads to an increase of the component parallel-β_j. This increase has oppositely directed consequences for the two instabilities involved. Whereas the growth rate of the EMIIC instability decreases, the threshold for the IC instability is lowered with increasing β. This reasoning remains valid even if an ion injection source for the backstreaming component were included. The effect of refreshing the backstreaming population with newly injected ions would be to keep the growth rate of the EMIIC instability constant at most. Additionally, when the rate of pitch angle scattering should decrease somehow, the constant driving effectively increases the temperature anisotropy, which soon will enforce growth of the IC instability again. So the net effect expected from driving at constant injection rates would be to sustain growth of the IC instability.

Nevertheless, more sophisticated simulations including injection sources are needed to clarify the importance of the EMIIC instability and the IC instability for the plasma sheet boundary layer.

Acknowledgements. M. Scholer would like to thank Y. Kamide for his kind hospitality at the Solar Terrestrial Environment Laboratory.

References

DeCoster, R. J., and Frank, L. A., Observations pertaining to the dynamics of the plasma sheet, *J. Geophys. Res.*, *84*, 5099, 1979.

Daughton, W., Gary, S. P., and Winske, D., Electromagnetic proton/proton instabilities in the solar wind: Simulations, *J. Geophys. Res.*, *104*, 4657, 1999.

Elphic, R. C., and Gary, S. P., ISEE observations of low-frequency waves and ion distribution function evolution in the plama sheet boundary layer, *Geophys. Res. Lett.*, *17*, 2023, 1990.

Gary, S. P., and Winske, D., Computer simulations of electromagnetic instabilities in the plasmasheet boundary layer, *J. Geophys. Res.*, *95*, 8085, 1990.

Matthews, A. P., Current advance method and cyclic leapfrog for 2-D multispecies hybrid plasma simulations, *J. Comp. Phys.*, *112*, 102, 1994.

Miura, A., Okuda, H., and Ashour-Abdalla, M., Ion beam driven ion cyclotron instability, *Geophys. Res. Lett.*, *10*, 353, 1983.

Weibel, E. S., Ion cyclotron instability, *Phys. Fluids*, *13*, 3003, 1970.

Winske, D., and Omidi, N., Electromagnetic ion/ion cyclotron instability at slow shocks, *Geophys. Res. Lett.*, *17*, 2297, 1990.

Winske, D., and Omidi, N., Electromagnetic ion/ion cyclotron instability: Theory and simulations, *J. Geophys. Res.*, *97*, 14779, 1992.